HIGH SENSITIVE H_2 GAS SENSOR OF ZnO/PS NANOSTRUCTURE PREPARED VIA PULSED LASER DEPOSITION TECHNIQUE

A. RAMIZY[a*], M. A. HAMMADI[a], I. M. IBRAHIM[b], M. H. EISA[c, d], R. ALHATHLOOL[d]

[a]*University of Anbar, College of Science, Department of Physics, Anbar - Iraq*
[b]*University of Baghdad, college of Science, Department of Physics, Baghdad- Iraq*
[c]*Physics Department, College of Science, Sudan University of Science Technology, Khartoum 11113, Sudan*
[d]*Department of Physics, College of Sciences, Al Imam Mohammad Ibn Saud Islamic University (IMSIU), Riyadh 11623, Saudi Arabia*

Porous Silicon (PS) has been prepared by electrochemical etching technique on the (111) P-type silicon wafer. The surface morphology of PS studied by atomic force microscope (AFM) verifies that the irregular and randomly distributed nanocrystalline silicon pillars and voids over the entire surface of silicon wafer. The average diameter was about 29.96nm and the average roughness about 0.747nm. The FE-SEM image of the PS sample showed a homogeneous pattern and confirms the formation of uniform porous structures on the silicon wafer. From XRD pattern, a broadening in diffraction peak was showed and the full-width at half maximum (FWHM) about 0.8951, crystalline size was found about 10.8nm. Photoluminescence spectra (PL) showed blue shift at 775nm (1.610eV). ZnO thin film was prepared by pulsed laser deposition technique deposited on slide glasses. The surface morphology of the film studied by (AFM), it is presented uniform distribution of densely packed of grains. The average diameter of ZnO film is 76.91nm and the roughness 1.88nm. FE-SEM images showed a fine-grained structure and unmodified without any cracks. It is observed that the ZnO particles are homogeneously dispersed in the PS surface. Structural properties of ZnO film investigated by XRD, the peaks appear belongs to hexagonal ZnO in (101) and (100) orientation. The crystalline size of the film is 17.8nm and 9.1nm, respectively. UV-V measurement showed that the energy gap (Eg) is equal to 3.4 eV. D.C. conductivity at the temperature (303-473) K for ZnO film showed that the film has two activation energies Ea1 (in the range from 303 to 383K) and Ea2 (in the range from 383 to 473K). Hall Effect measurements showed that the film has n-type charge carriers with concentration of $25.131x10^{14}cm^{-3}$ and mobility of $1.03cm^2/v.sec$. ZnO/PS gas sensor showed very high sensitivity for H_2 gas is about 15575.0% in 350 ˚C and a shorter time response about 15.5s

(Received October 16, 2016; Accepted December 14, 2016)

Keywords: High sensitive; PLD; ZnO/PS; H_2 Gas sensor

1. Introduction

Zinc oxide (ZnO) is an II-VI semiconductor with wide and direct band gap semiconductor with 3.3 eV band gap which crystallizes in the hexagonal wurtzite structure [1]. It has a very large exciton binding energy of 60meV at room temperature [2], including excellent chemical and thermal stability. ZnO is useful in various technological domains such as transparent electrodes, solar cell, gas sensors, light emitting diodes, the active channel in thin films transistor and optoelectronic devices. It has been widely used for optical, electrical, optoelectronic, catalytic, and photochemical properties, including optical waveguides and transparent conducting coatings [3]. Many techniques have been used to deposit the thin film, the deposition techniques are broadly classified into two categories, viz. physical methods and chemical methods.

*Corresponding author: asmat_hadithi@yahoo.com

Chemical bath deposition, chemical vapor deposition, and spray pyrolysis are examples of the chemical method of thin film deposition. Thermal evaporation, e- beam evaporation, Rf and Dc sputtering and pulsed laser deposition (PLD) are examples of physical methods of thin film preparation [4]. The method used in in this research the technique pulsed laser deposition (PLD). This technique has many advantages such as, (a) is that complex materials can be easily ablated with fast response, (b) the composition of the films grown by PLD is quite close to that of the target, (c) the surface of the films is very smooth, (d) good quality films can be deposited at room temperature due to high kinetic energies (>1 eV) of atoms and ionized species in the laser produced plasma [5].

In this work, PLD technique is used to deposit ZnO pure and doped by Eu^{+3} on substrates glass and porous silicon to get the device. Porous silicon (PS) is one of the most promising material; it can emit the visible range of light at room temperature. Porous silicon (PS) has many unique characteristics such as direct and wide modulated energy band gap, high resistivity, and the same single-crystal structure as bulk. PS absorbs light more strongly than bulk silicon [6].

In general porous silicon (PS) obtained by anodization of a silicon wafer is a versatile material which can display different morphologies by varying the doping density of the wafer as well as the formation parameters. PS can be prepared by different techniques such as photochemical, electrochemical, photo-electrochemical, **s**tain etching processes, and laser induced etching process [7]. One of the most important methods is electrochemical etching process. Many parameters that influence on the PS formation process with electrochemical anodization such as substrate doping, current density, HF concentration, and time etching [8, 9]. The film based gas sensors depending on the detection of variation in some electrical parameter, resistance or capacitance, of the film utilize n-type semiconducting metal oxides such as ZnO. Also, metal oxides are stable at increased temperatures in air [10]. In this paper, structural, optical, electrical and morphological properties of ZnO thin film prepared by PLD techniques along with H_2 gas sensing has been presented.

2. Experimental procedure

2.1. Preparation of Pellets

ZnO powder with a high purity of 99.999% was pressed it under 5 ton and for 3-5 minutes at room temperature to form a target in 1.2 cm as a diameter and 0.2 cm as a thickness. It should be dense and homogenous as possible to ensure a good quality of the deposit.

2.2. Substrates Preparation

There are two substrates used in this work glass and PS. For the glass substrate, the slides were cleaned by distilled water and then rinsed in the ultrasonic unit for 10 minutes, then replacing the distilled water with a pure alcohol solution and put it again in ultrasonic unit for 10 minutes to remove any organic contaminant and residual particles on it. After then the slides dried by blowing air and wiped with soft tissue. For PS substrates, P-type Si wafers with <111> orientation cut into pieces at area of $1cm^2$. Silicon samples were cleaned by acetone and methanol to remove the native oxide layer and the other impurities. Si samples put on the bottom of the cell (electrochemical etching process (ECE) as shown in Fig. 1) by using O-ring that allowed the Si surface to be exposed to the homogeneously mixed of HF: ethanol at 1:1 concentration. Si wafers connected to the anode electrode and the Platinum connected to the cathode electrode of the power supply with an etching time 20min and current density about $10mA/cm^2$.

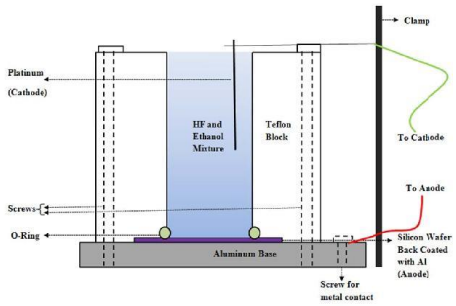

Fig. 1 Schematic of the electrochemical etching

2.3. Thin Film Preparation

ZnO thin film was based on (PS and glass) substrates were deposited by pulsed laser deposition (PLD) technique with 300mJ and 300pulsed. The experiment was carried out inside a vacuum chamber generally at (10^{-3} Torr) vacuum conditions, Fig. 2 shows the arrangement of the target and substrate holders inside the chamber with respect to the laser beam. Nd: YAG laser. The laser characterizations are a model (Q-switched Nd: YAG Laser Second Harmonic Generation (SHG)), with two wave lengths of 1064,532 nm, pulse duration of 10 ns, Repetition frequency 6 Hz, Cooling method: inner circulation water cooling and Power supply of 220V. The samples prepared at laser energy about 300mJ with 300 pulsed.

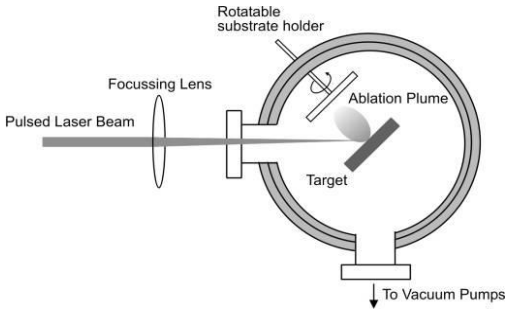

Fig. 2 Diagram of the pulsed laser deposition set up.

3. Results and discussion

Fig. 3a shows the AFM 3D image of PS surface etched at the current density of 10mA/cm^2 and time about 20min. A sponge-like structure is produced, in which the irregular and randomly distributed nanocrystalline silicon pillars and voids over the entire surface of silicon wafer. The average diameter was about 29.96nm and the average roughness about 0.747nm. Figure 3b is the image of pure ZnO thin film; it is presented a uniform distribution of densely packed of grains. The average diameter of pure ZnO film is 76.91nm and the roughness 1.88nm.

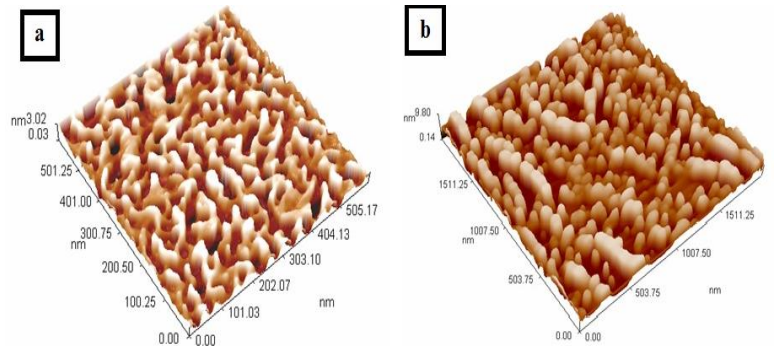

Fig. 3 AFM images of: a) PS prepared by ECE technique with a time 20 min. and current density 10mA/cm^2. b) Annealed ZnO film prepared by PLD technique with laser energy 300mJ and 300 pulsed.

Fig. 4a shows FE-SEM image for PS was prepared it shows a homogeneous pattern and confirms the formation of uniform porous structures on the silicon wafer. Fig. 4b illustrate the surface morphology of ZnO/PS film by FE-SEM image and show a fine-grained structure and unmodified without any cracks. It is observed that the ZnO particles are homogeneously dispersed in the PS surface.

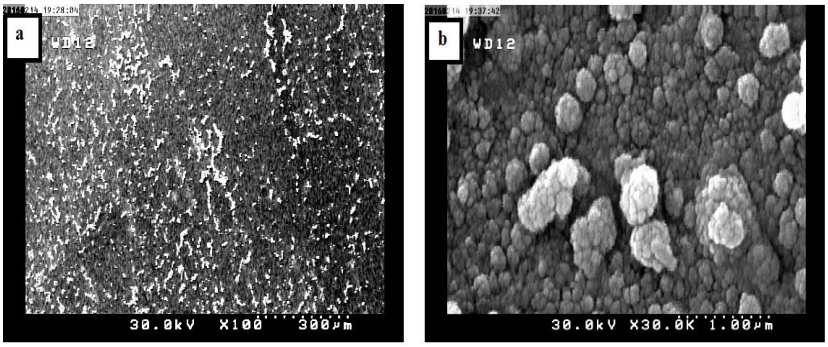

Fig. 4 FE-SEM image of a) PS sample b)ZnO film prepared by PLD technique with laser energy 300mJ and 300 pulsed

Fig. 5a shows X-ray diffraction analyses of the PS sample were carried out in the 10˚-100˚ range of 2θ. The figure exhibited two interesting peaks of the sample was prepared, one prominent and sharp peak was found at 2 θ = 27.6^o and another one, weaker than the former, at 2 θ =93.9˚. The founded values correspond to (111) and (151) c-Si orientations, respectively. For the strong peak (111), the crystalline size, which is the representation of the remnant silicon portion after the dissolution and formation of pores [11], was measured by using Scherrer equation [12]:

$$G.S = \frac{0.94\lambda}{\beta.\cos(\theta)} \quad (1)$$

where θ is the Bragg angle, λ the X-ray wavelength, the constant quantity 0.94 represented Scherrer's constant, and β is the full width half maximum (FWHM) of X-ray peak and it was found about 10.8nm and full-width at half maximum (FWHM) about 0.8951. These computed results have been compared with the FWHM values of Cu-Kα which have been published by Joint Committee on Power Diffraction Standards (JCPDS) the FWHM of bulk silicon about 0.295. A broadening of diffraction peaks was observed, which confirms the formation of pores on the crystalline silicon surface. The presence of this peak in the PS structures confirms that the cubic structure of the crystalline silicon is retained even after the pore formation [11]. Figure 5b shows

the well crystalline hexagonal structure in ZnO film. Two peak appears at 2Θ=35.832° and 31.481° with 101 and 100 orientations respectively. These observed values are in good agreement with standard values. FWHM of the two peaks is about 0.4686 and 0.9038, respectively. The crystalline size of the two peaks is calculated from equation 1 and the results were found about 17.8nm and 9.1nm respectively.

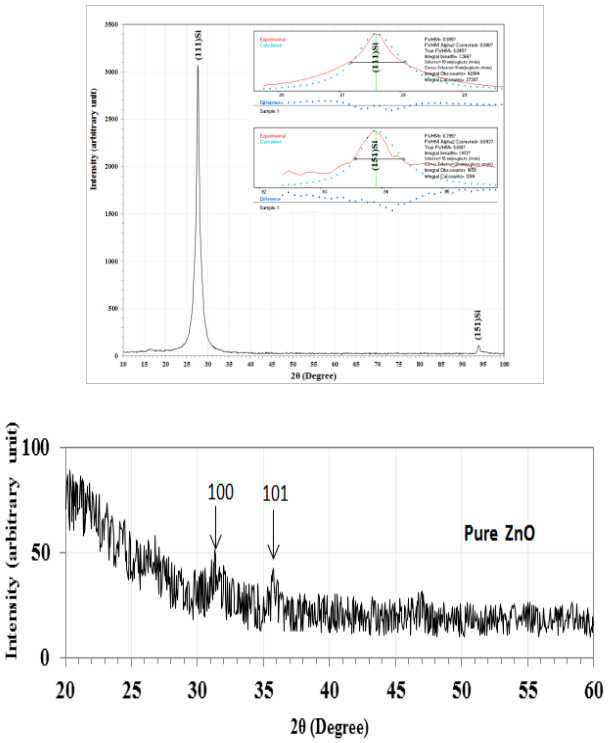

Fig. 5 XRD spectra of: a) PS etched with a current density of 10 mA/ cm^2 and with time 20min. b) Pure ZnO thin film

Fig. 6 shows the PL spectra for PS sample; peak position was located at 770nm. Energy gap Eg was calculated from the equation [13]:

$$\lambda(\text{nm}) = \frac{1240}{E_g(\text{eV})} \quad (2)$$

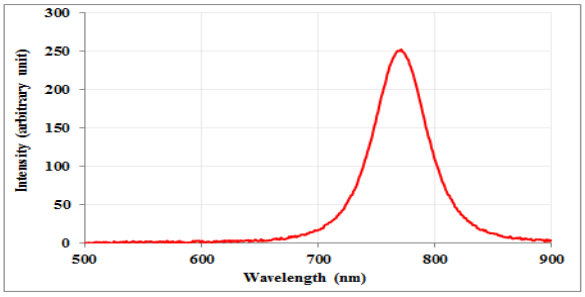

Fig.6 PL spectra of PS etched for 20 min and 10mA/cm^2.

Eg of PS was found about 1.610eV while for wafer Si is about 1.12eV. The PL peak position of PS is blue-shifted, according to the quantum confinement model; the peak shift is due to an increase in the energy band gap (Eg) within the porous structure. This is attributed to the reduction of the Si to nanosize, which favors charge carrier quantum confinement [14].

Fig. 7a and 7b shows the UV–Vis transmission and absorption spectra of the as-prepared un-doped ZnO sample deposited with laser energy 300mJ and 300 pulses. The transmittance in the visible part of the spectra (400-700) nm showed a high value about 88% at λ equal to 500nm and the absorption coefficient about 13198 cm^{-1}.

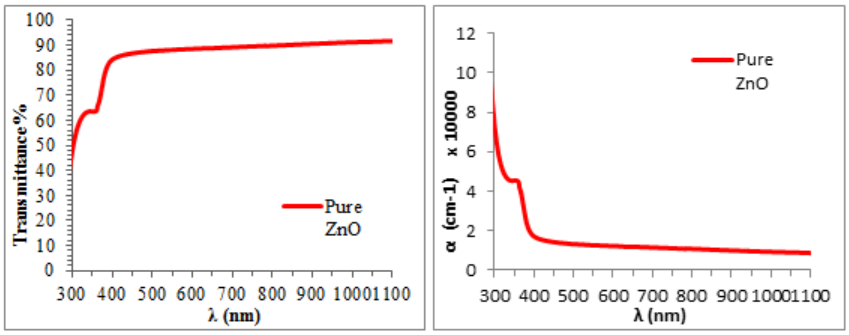

Fig. 7 a) Optical transmittance spectra of pure ZnO b) Absorption coefficient spectra of pure ZnO

Fig. 8 represents the calculation of Eg of un-doped ZnO by using equation 2, the band gap is calculated by extrapolating a straight line to the abscissa axis. When α is zero, then Eg = hν. The results showed that the energy gap is equal to 3.4eV.

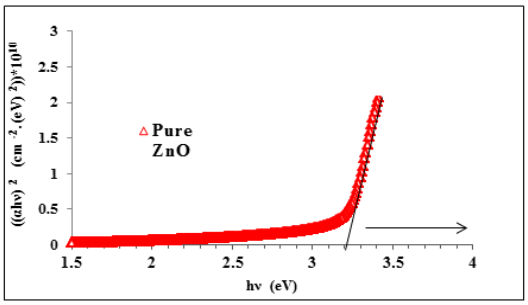

Fig.8 The variation of $(\alpha h\upsilon)^2$ versus photon energy (hυ) for ZnO film.

Fig. 9 shows D.C conductivity for un-doped ZnO films deposited by PLD with 300 mJ and 300 pulses. The sample measured in the temperature range 303K-473K, the conductivity and the activation energy measured by using equations [15]:

$$\sigma = \frac{L}{R.A} \tag{3}$$

$$\sigma = \sigma_{\circ} \exp\left[\frac{-E_a}{k_B T}\right] \tag{4}$$

Where L is the electrodes separation, R is the resistance and A is the cross-section area of the sample σ_o is minimum conductivity, E_a is the activation energy equals ($E_c - E_F$), k_B is Boltzmann's constant and *T* is the absolute temperature in Kelvin.

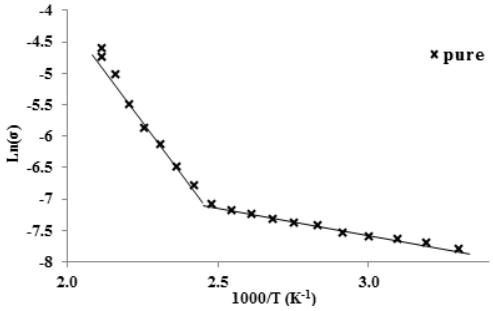

Fig. 9 Variation of Ln (σ) with reciprocal temperature for ZnO film.

The results indicate that the film has two activation energies Ea1 (in the range from 303 to 383K) and Ea2 (in the range from 383 to 473K). The value of Ea1 is equal to 0.069eV and Ea2 is 0.486eV.

From Hall measurements, the carrier concentration (n_H) and carrier mobility (μ_H) values of ZnO thin were calculated. The negative sign of Hall coefficient indicates the conductivity nature of the film is n-type, the carrier concentration is $25.131\times10^{14}cm^{-3}$ and the mobility 1.03 cm^2/v.sec.
Fig. 10 show the resistance of the ZnO pure based on PS substrate as a function of time with on/off gas valve exposed to 3% concentration of H_2 gas at 200, 250, 300, and 350 °C. The resistance decreases when the gas valve is on, however, the resistance is increased rapidly when the gas is off. To explain this case, under an air atmosphere the molecules can get adsorbed on the surface semiconductor and extracts electrons from the conduction band to form oxygen ions. That may lead to the formation of an electron depletion region near the surface, which can greatly increase the resistance due to the decrease of net carrier density. When the sensor is exposed to a hydrogen atmosphere, the hydrogen molecules will react with the adsorbed oxygen species. The redox reaction is exothermic and results in the fast desorption of produced H_2O molecules from the surface. The released electrons will reduce the thickness of the depletion region, and decrease the resistance of the semiconductors. When the sensor is exposed to the air ambient again, the depletion region will be rebuilt by adsorbed oxygen species. The resistance will regain the initial level before hydrogen response [16].

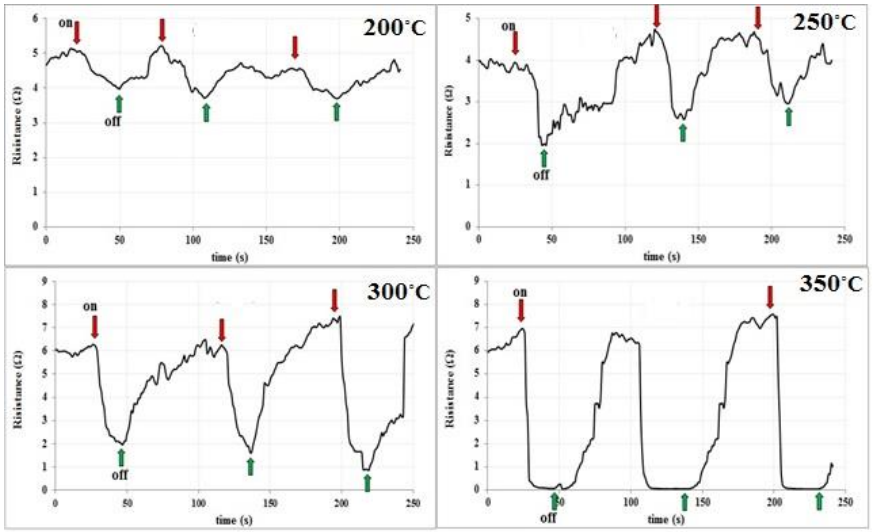

Fig. 10 Resistance of ZnO/PS as a function of time at different operating temperatures for H2 gas.

Table 1 shows the sensitivity values of pure ZnO for 3% ratio of H_2 gas was calculated from equation [17]:

$$S = [R_{air} - R_{gas}]/R_{gas} \quad (5)$$

With different temperatures (range 200-350 ˚C at increments of 50 °C). It was shown that the sensitivity of ZnO films increases with the increasing in the operating temperature, reaches a maximum value about 15575.0% corresponding to an optimum operating temperature which is 350°C for the sample. To determine the optimum operating temperature of this sensor, after exposure of the sample to 3% of H2 gas, the resistance decreased, and then increased rapidly with outage of H2 gas. This observed behavior may be explained as follow Liu et al. (2005) and Khojier et al. (2015) [18; 19]: as a consequence of reaction of hydrogen with oxygen of the surface of ZnO thin film water molecules and oxygen vacancies are formed which in turn cause electrons to be transferred to the conduction band, hence reducing the resistance of the sample/sensor. When the sensing chamber is purged with air the vacancies formed in the aforementioned process will be occupied by oxygen which in turn cause electrons to be captured from the conduction band, hence the resistance of the sensor increases [20].

Table 1 Gas sensor parameters (sensitivity, time response and time recovery) for ZnO thin film based on PS exposed to 3% ratio of H_2 gas.

Sample	Temperature (° C)	sensitivity %	response time(s)	recovery time(s)
Pure ZnO	200	34.5	20.0	25.0
	250	93.7	16.7	24.5
	300	737.7	19.5	47.1
	350	15575.0	15.5	39.6

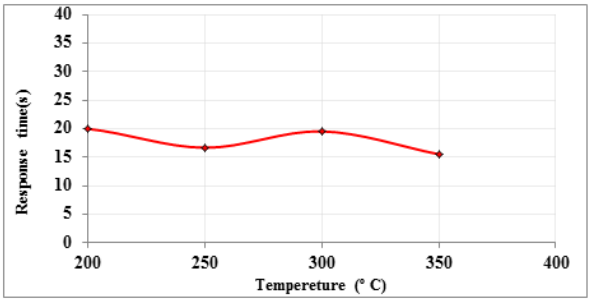

Fig. 11 The variation of response time with the operating temperature of ZnO film based on PS for H_2 gas.

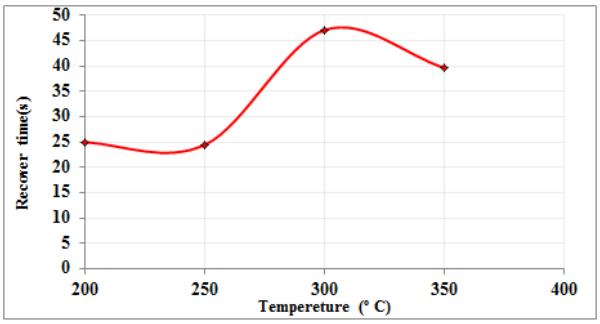

Fig. 12 The variation of recovery time with the operating temperature of ZnO film based on PS for H_2 gas.

Fig. 11 and 12 shows the relation between the response time and the Recovery time as a function of operation temperature for ZnO thin film based on PS substrate. The results obtained that the response time decreases with increasing the operation temperatures and showed the shorter time response about 15.5s at 350 ˚C. The time response is a very interesting parameter in the gas sensor device in addition to the sensitivity.

In general, the small-sized nanoparticles decrease the response time and increase the sensitivity of the ZnO nanostructure -based gas detectors [21]. The reduction of the grain size that leads to faster oxidation of gas which particularly reduces the work function and the activation energy of surface reaction may be associated with an increase in oxygen vacancies created upon ZnO lattice. In real situations, a fast response time is usually required, but a fast recovery time is not so important, and recovery time decreases above optimal time with increases temperature.

4. Conclusions

AFM images of PS showed A sponge-like structure is produced, in which the irregular and randomly distributed nanocrystalline silicon pillars and voids over the entire surface of silicon wafer. FE-SEM image of PS showed a homogeneous pattern uniform porous structure. XRD pattern of PS shows a broadening in diffraction peaks which indicate forming of nanostructure shapes. PL peak position of PS is blue-shifted, according to the quantum confinement model; the peak shift is due to an increase in the energy band gap (Eg) within the porous structure. This is attributed to the reduction of the Si to nanosize, which favors charge carrier quantum confinement.

The values of grain size were recorded of ZnO thin film in glass substrate indicate that the structure of grains is in nanoscale, the film is in (101, 100) orientations and belongs to wurtzite ZnO. Pure ZnO has high transmission and large Eg. The results of D.C conductivity showed that the film, have two activation energies. From Hall measurement, the film of ZnO has the n-type carrier. For Pure ZnO thin film deposited on PS, FE-SEM image showed a homogeneous pattern as a fine-grained structure and unmodified without any cracks. It is observed that the ZnO particles are homogeneously dispersed in the PS surface. In different operation temperature, ZnO/PS has the best sensitivity for H_2 gas and a short time response in 350˚C.

Acknowledgements

Authors are grateful to the Department of Physics, Collage of Science, Anbar and Baghdad University, Iraq. The authors would like thank friends for generous support and for valuable discussions and comments.

References

[1] S. Christoulakis, M. Suchea, E. Koudoumas, M. Katharakis, N. Katsarakis, et alApplied Surface Science, **252**, 5351 (2006).
[2] B. Mukherjee, "Synthesis, Structural, Optical and Electrical Properties of Zinc Oxide nanoparticles," MSc. Thesis, Indian Institute of Technology Madras, (2009).
[3] A. Phuruangrat, O. Yayapao, T. Thongtem, and S. Thongtem, Journal of Nanomaterials, **2014**, 9 pages. (2014).
[4] R. Manoj, "Characterization of Transparent Conducting Thin Films Grown by Pulsed Laser Deposition and RF Magnetron Sputtering," Ph.D. thesis in the field of material science, Cochin University of Science and Technology, India, (2006).
[5] B. D. Chrisey, and G. K. Hubler (Eds), "Pulsed Laser Deposition of Thin Films," Wiley, New York, (1994).
[6] K. Lee, Y. Tseng, C. Chu, Applied Physics, **67**(5), 541 (1998).
[7] P. Malempati, "Surface-Enhanced Raman Spectroscopy Substrates Based on Nanoporous Silicon and Pattern Transfer," M.Sc. Thesis. Louisiana State University, USA, (2011).

[8] E. X. Pérez, "Fabrication and Characterization of Porous Silicon Multilayer Optical Devices," University Rovera, (2007).
[9] G. X. Zhang, Jour. of Electroch. Soci., Mississauga, Canada, **151**, 65 (2003).
[10] S. Dixit, A. Srivastava, R. K. Shukla, Journal of Applied Physics **102**(11),Article ID113114 (2007),
[11] M. Jayachandran, M. Paramasivam, K.R. Murali, D.C. Trivedi, M. Raghavan, Mater.Phys.Mech. **4,** 143 (2001).
[12] L. L. Yang, "Synthesis and Optical Properties of ZnO Nanostructures," Linköping University, Sweden, (2008), p. 32.
[13] J. Millman, A. Grabel, "Microelectronics," New York: McGraw-Hill, (1987).
[14] A. R. Abd-ALghafour, "Nanostructured Porous Si and GaN Fabricated by Electrochemical and Laser Induced Etching Techniques," University Sains, Malaysia, (2011), P.65-90
[15] B. G. Streetman, "Solid State Electronic Devices," Semiconductors, 2nd Ed. Englewood Cliffs, (1980).
[16] H. Gu, Z. Wang, Y. Hu, Sensors, **12**, 5517 (2012).
[17] Abu Z. Sadek, S. Choopun, W. Wlodarski, S. J. Ippolito, K. Kalantar-zadeh, IEEE Sensors Jour. **7**(6), 919 (2007).
[18] Y. Liu, J. Dong, P.J. Hesketh, M. Liu Journal of Materials Chemistry, **15**, 2316 (2005).
[19] K. Khojier, H. Savaloni, Journal of Electronic Materials, DOI: 10.1007/s11664-015-3833-2. (2015),
[20] F. Teimoori, K. Khojier, N.Z. Dehnavi, Science Direct, Procedia Materials Science, **11**, 474 (2015).
[21] A. Erol, S. Okur, B. Comba, Ö. Mermer, M.C. Arıkan, Sensors and Actuas B: Chem. **145**(1), 174 (2010).